



Development of a reaction-sintered silicon carbide matrix composite

A. Sayano^{a,*}, C. Sutoh^a, S. Suyama^a, Y. Itoh^a, S. Nakagawa^b

^a Heavy Apparatus Engineering Laboratory, Toshiba Corporation, 2-4 Suehiro-cho, Tsurumi-ku, Yokohama 230, Japan

^b Nuclear Fusion Development Department, Toshiba Corporation, 1-1-6 Uchisaiwai-cho, Chiyoda-ku, Tokyo 100, Japan

Abstract

SiC matrix composites reinforced with continuous SiC-based fibres using reaction sintering (RS) for matrix processing were produced and their mechanical and physical properties were studied. Mechanical behaviour of SiCf/SiC (RS) composites in tension and in flexure exhibits improved toughness and a non-catastrophic failure due to fibre crack bridging and pullout from the matrix, and the composites exhibit high thermal conductivity, high Young's modulus and reduced porosity. Moreover, SiCf/SiC (RS) composites showed improved thermal shock resistance in comparison to monolithic RS-SiC. SiC matrix processing by RS leads to reduced production times and lower costs when compared with other methods such as polymer impregnation and pyrolysis (PIP) or chemical vapour infiltration (CVI). Composite prototypes were also produced for feasibility demonstration, and it was verified that the method could be applied to produce large parts and complex shapes. © 1999 Elsevier Science B.V. All rights reserved.

1. Introduction

SiC continuous fibre-reinforced SiC matrix composite (SiCf/SiC) is being developed as a potential material for high-temperature energy applications such as gas turbines, heat exchangers or gas filters [1–5]. In particular, because of its high-temperature stability, high-temperature strength and damage tolerance, considerable attention is being paid to the gas turbine applications including moving blades, stator blades and combustors. SiC-based composites are also considered promising material for nuclear fusion applications due to their low radioactivation, high damage tolerance, high stability at high temperatures, high thermal conductivity and so on.

Current fabrication processes for SiCf/SiC Polymer Impregnation and Pyrolysis (PIP) [6,7] and Chemical Vapour Infiltration (CVI) [8,9]. In the first, the fibre preform is impregnated with a polymer precursor, SiC powder and organic solution such as xylene, followed by curing and high-temperature pyrolysis. Several impregnation and pyrolysis cycles, up to 10, may be required to

achieve an acceptable density. In the case of the CVI production route, SiC matrix is obtained by infiltrating a reactant gas (e.g., methylchlorosilane) at high temperatures, into the fibre preform.

The reaction sintering process for SiCf/SiC composite considered here is unique and totally different from the above two methods [10–14]. A slurry consisting of a mixture of SiC powder and carbon powder in water is impregnated into the SiC fibre preform. The obtained green composite is finally reaction-sintered with the melted silicon, to obtain a rich SiC matrix.

In this work, mechanical and thermophysical properties of the reaction-sintered SiCf/SiC composite are reported and the merits of the process are discussed in comparison with other typical processes such as PIP and CVI. Further, some prototypes manufactured by reaction sintering are presented and the advantages of this production route are also discussed.

2. Experimental

In Fig. 1, the production steps of the SiCf/SiC (RS) composite are described. The SiC fibres used were Hi-Nicalon (Nippon Carbon, Japan) previously coated

* Corresponding author. Tel.: +81-45 510 5200; fax: +81-45 500 1423.

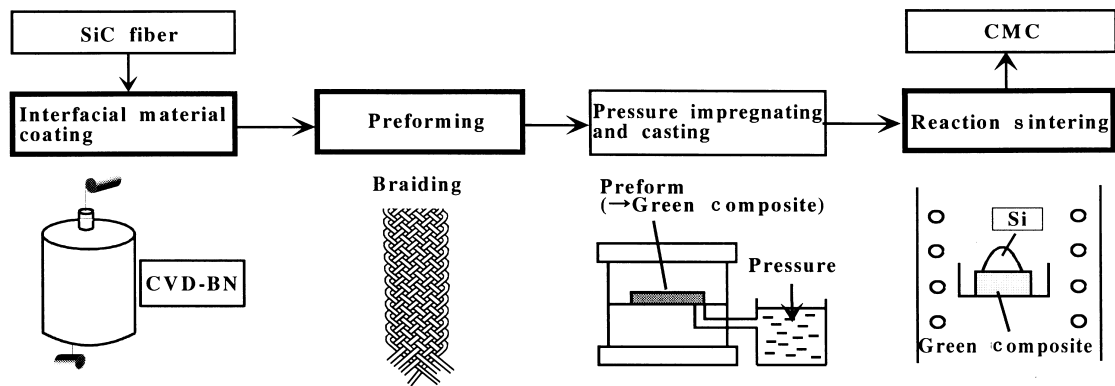


Fig. 1. Fabrication process of SiCf/SiC composite.

with boron nitride using Chemical Vapour Deposition (CVD). Fibre bundles consisting of 2000 filaments (average diameter of the fibre is 14 μm) were braided and reinforcement cloths consisting of 13 bundle units were obtained. One layer of fibrous preform was then set in a porous mould, and green composites were obtained by slip impregnation and casting of a matrix slurry. This slurry consists of a mixture of SiC and C powders, dispersant in water. After drying, the green composites were reaction sintered in vacuum, at 1720 K, for 5 h in contact with melted silicon.

Mechanical and thermophysical properties were evaluated for SiCf/SiC (RS) composite. The strength was evaluated by a three-point bending test and by a tensile test. The sample size for both tests was $40 \times 10 \times 1 \text{ mm}^3$. Displacement was measured by the strain gauge set on the samples in the tensile test. Young's modulus was calculated by the displacement and the load, and Poisson's ratio was calculated by the displacement values of the two directions, perpendicular and parallel to the tension. The thermal conductivity was calculated by the thermal diffusion rate and the specific heat. These values were measured by a laser flash method at room temperature and at 1000°C by using disc-shaped specimens whose dimensions were 10 mm(diameter) \times 1.2 mm(thickness). The coefficient of thermal expansion was measured from room temperature to 1300°C by the compressive load method. Aluminium electrodes were formed for the samples and current-voltage characteristics were measured.

Thermal shock test was carried out for both monolithic reaction sintered SiC and SiCf/SiC (RS) composite. Fig. 2 shows the schematic representation of the thermal shock test. The test sample size was $20 \times 20 \times 2.5 \text{ mm}^3$. The samples were held in the furnace for 30 min at different temperatures from 200°C to 900°C and were then quenched in water. After testing, the appearance and the microstructure of the samples were observed by visual inspection and SEM.

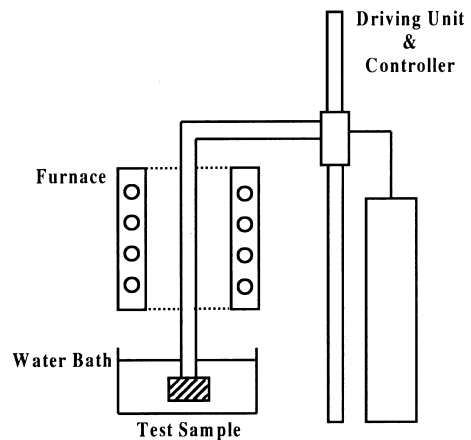


Fig. 2. Schematic representation of thermal shock test.

A plate ($140 \times 140 \times 6 \text{ mm}^3$) and an octagonal sleeve (Φ : 70 mm, height: 50 mm, thickness: 3 mm) were manufactured as prototypes. The fabrication process is similar to that of the test samples referred to in Fig. 1. In the case of the plate, coated filaments were woven to form a two-dimensional plane cloth and the preforms were laid and set in the porous mould. For the sleeve prototype, the filament yarns were braided to a core material. After slurry impregnation and subsequent drying, the core material was removed and the dried green composite was submitted to the subsequent steps to obtain the composite component.

3. Results and discussion

Table 1 shows the properties of the sintered composite by the reaction sintering process. For comparison, typical properties of the material made by PIP and CVI are also presented [15]. As the type of fibre, the fibre

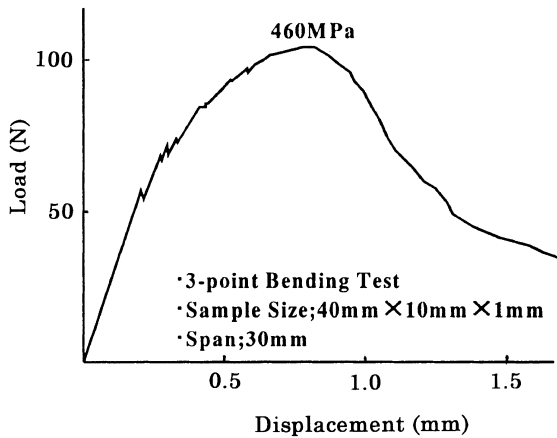


Fig. 3. Typical load–displacement curve of SiCf/SiC composite.

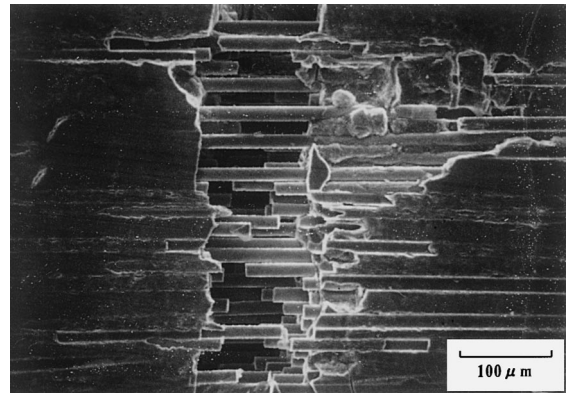


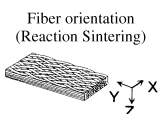
Fig. 4. Crack opening region following three-point bending test.

volume fraction and the fibre orientation are different among these composites, only qualitative comparison is possible, but it is evidenced that the reaction sintering process permits to obtain a material with low porosity, high thermal conductivity and high Young’s modulus, when compared to composites produced by PIP and CVI. Reduced porosity and high thermal conductivity is

especially advantageous for nuclear applications. The reason for the exhibited low porosity relies on the unique sintering process in which silicon-melt reacts with the carbon powder in the matrix slurry, so that SiC is formed and the pores present in the green composite are filled with the melted silicon. The residual silicon metal in the matrix of the composite is 15–20 vol% after

Table 1
Properties of SiCf/SiC composite

Process	Reaction bonding	PIP (polymer impregnation and pyrolysis)	CVI (chemical vapour infiltration)
Structure			
Fiber	Hi-Nicalon	Nicalon	Nicalon
Fiber volume fraction	30% (braid)	30% (cloth laminate)	40% (cloth laminate)
Density	3.0 g/cm ³	1.9 g/cm ³	2.6 g/cm ³
Porosity	~2%	~23%	8–15%
Properties			
Heat resistant temperature	1350°C	1000°C	1200°C
Young’s modulus	240 GPa	50 GPa	230 GPa
Tensile strength	500 MPa	110 MPa	200 MPa
Poisson’s ratio	0.2	–	–
Thermal conductivity	50 W/m K (RT) 30 W/m K (1000°C)	0.56 W/m K (500°C) 0.73 W/m K (700°C)	9.7 W/m K (RT) 6.2 W/m K (1000°C)
Coefficient of thermal expansion	4.9 × 10 ⁻⁶ K ⁻¹ (Y-direction) 4.7 × 10 ⁻⁶ K ⁻¹ (X-direction), RT – 1300°C	3.6 × 10 ⁻⁶ K ⁻¹	3 × 10 ⁻⁶ K ⁻¹ () 2.5 × 10 ⁻⁶ K ⁻¹ (⊥)
Resistivity	13 Ω cm (Y-direction) (at 1 A/cm ²) 0.7 Ω cm (Z-direction)	–	–
Characteristic	Productivity; good complicated shape; possible cost; low	Productivity; not bad complicated shape; possible cost; not high	Productivity; not good complicated shape; possible cost; high



sintering. The amount of residual silicon is chiefly controlled by the slurry component and the packing density of the matrix powder in the fibre preform. The improved thermal conductivity is considered to be related to the low porosity. In terms of electrical resistivity, the effect of the fibre orientation and non-linear V–I relation were observed.

SiCf/SiC composites produced by reaction sintering are also advantageous with regard to production costs and processing times. Production routes such as PIP and CVI which make use of polymer precursors (liquid or gaseous reactants) are quite expensive, while low-cost SiC and carbon powders are utilized to obtain the slurry in the reaction sintering process. Moreover, PIP requires several impregnation and pyrolysis cycles, up to 10, in order to achieve acceptable density of the final composite. Also CVI requires extensive time for deposition of the SiC matrix in the fibrous preform. These large production times are not necessary for reaction sintering, as only one cycle of slurry impregnation and sintering is required, to obtain SiCf/SiC composites. Fig. 3 shows the typical load–displacement curve at room temperature in a three-point bending test. Ultimate strength shows 460 MPa and non-brittle failure is observed. It is also evident that the discontinuity of the curve is for the stress value around 200 MPa, which is considered to correspond to the initial matrix cracking. The point of this initial matrix cracking of the composite is high compared to the one made by the PIP and CVI methods, where crack initiation is said to be below 100 MPa.

Fig. 4 shows the crack opening region following the three-point bending test. Fibre bridging between the matrix and fibre pull-out from the matrix account for the non-catastrophic failure are observed.

Table 2 shows the thermal shock test results. In this table, the crack refers to those distinguishable by visual observation, while microcrack identifies those discerned only by microscope observation. In the case of monolithic reaction-sintered SiC, cracks were observed for the samples which were quenched into the water for the temperatures above 600°C, whereas in the case of the composites, cracks were not observed for all the samples in this test. However, according to microscope obser-

Table 2
Thermal shock test results

Holding temperature (°C)	Monolithic (RB-SiC)		CMC (SiCf/RB-SiC)	
	Micro crack	Crack	Micro crack	Crack
200	none	none	none	none
400	exist	none	exist	none
600	exist	exist	exist	none
800	exist	exist	exist	none
900	exist	exist	exist	none

vation, microcracks were observed for the samples which were quenched into the water for the temperatures above 400°C for both composite and monolithic materials. Fig. 5 shows an example of a visual observation in the thermal shock test (900°C → water). Fig. 6 shows an example of a microstructure in the composites after the thermal shock test. It is noticed that the progress of the microcrack is stopped by the fibre.

In Fig. 7, prototypes manufactured by the reaction sintering are presented. Shrinkage of green composite during reaction sintering is negligible, by which the movement of the filaments during reaction sintering is near zero, accordingly the matrix sintering could smoothly proceed without the interference of the fibre preform. This is advantageous for preventing crack occurrence in the matrix, and is very important for manufacturing CMC products. It has been confirmed that

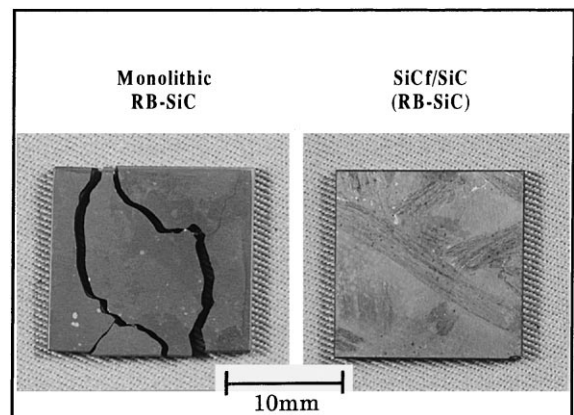


Fig. 5. Thermal shock test results (900°C → water).

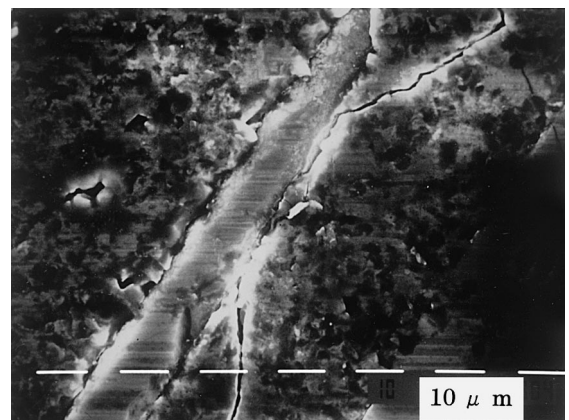


Fig. 6. Microstructure of SiCf/SiC composite after thermal shock test.

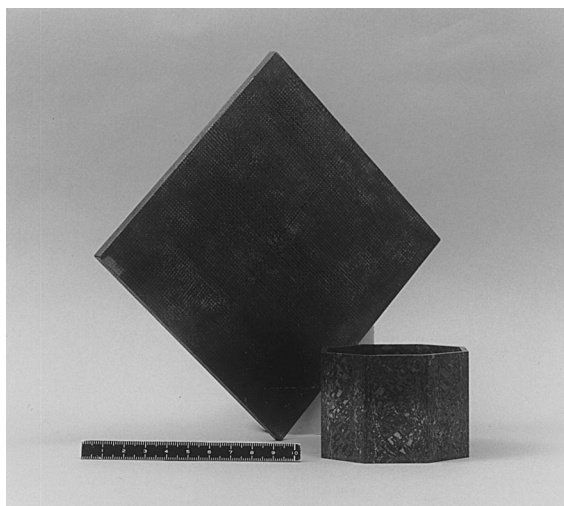


Fig. 7. SiCf/SiC composite prototypes.

the process can be applicable to large and complicated parts.

In order to meet specific requirements for fusion applications, several issues for current SiCf/SiC (RS) composite will be addressed in the future. These includes optimization of the fibre/matrix interface, as boron nitride is detrimental in a fusion environment, in particular, nitrogen will lead to the production of ^{14}C , thus reducing the potential low-activation features of SiC-based materials. Furthermore, a careful assessment of the impurity content must be carried out, similar to that carried out for SiCf/SiC (CVI) composite for an integral qualification of the low-activation features of SiCf/SiC (RS) [16]. Improvements on the fibre architecture ap-

propriate to the needs of particular parts and on the techniques to produce complex fibre preforms are also necessary, in order to permit production of large components and different shapes. Finally, optimization of the impregnation and sintering process will improve reproducibility and overall improvement of the properties of the composite.

References

- [1] K.L. Luthra, R.N. Singh, M.K. Brun, *Am. Ceram. Soc. Bull.* 72 (7) (1993) 79.
- [2] G.S. Corman, J.T. Heinen, R.H. Goetze, *Am. Soc. Mech. Eng.* 95-GT-387 (1995).
- [3] K. Park, T. Vasilos, *J. Mater. Sci. Lett.* 15 (1996) 8.
- [4] P. Pluvinage, A. Parvizi-Majidi, T.W. Chou, *J. Mater. Sci.* 31 (1996) 232.
- [5] K. Park, S.G. Dipietro, G.S. Thurston, *J. Mater. Sci. Lett.* 15 (1996) 1743.
- [6] S. Riccitiello, *J. Adv. Mater.* 1 (1994) 22.
- [7] J. Gotoh et al., in: *Proceedings of the Fourth Japan International SAMPE Symposium, 1995*, pp. 240–245.
- [8] D.P. Stinton et al., *J. Mater. Sci.* 30 (1995) 4279.
- [9] Y. Ohzawa, M. Takahashi, K. Sugiyama, *J. Mater. Sci.* 32 (1997) 4289.
- [10] T. Kameda et al., in: *Proceedings of the Fourth Japan International SAMPE Symposium, 1995*, pp. 252–257.
- [11] A. Sayano et al., in: *Proceedings of the Fourth Japan International SAMPE Symposium, 1995*, pp. 258–263.
- [12] N. Amiji et al., *Japan Ceram. Soc. Bull.* 31(7) (1996) 567.
- [13] T. Kameda et al., in: *Proceedings of the Joint Canada–Japan Workshop on Composites, 1996*, p. 33.
- [14] N. Amiji et al., in: *The Third International Symposium on New Textiles for Composites, 1996*.
- [15] H. Ichikawa, *Japan J. Radiat. Chem.* 58 (1994) 21.
- [16] H.W. Scholz et al., *J. Nucl. Mater.* 21–215 (1994) 655.